crystals

MDPI

Review

Ionic Conductors: Effect of Temperature on Conductivity and Mechanical Properties and Their Interrelations

Masaru Aniya [1,*], Haruhito Sadakuni [2] and Eita Hirano [2]

[1] Department of Physics, Faculty of Advanced Science and Technology, Kumamoto University, Kumamoto 860-8555, Japan
[2] Department of Physics, Graduate School of Science and Technology, Kumamoto University, Kumamoto 860-8555, Japan; thrhnkds@yahoo.co.jp (H.S.); eita.hirano07@gmail.com (E.H.)
* Correspondence: aniya@gpo.kumamoto-u.ac.jp

Abstract: The ionic transport and the mechanical properties in solids are intimately related. However, few studies have been done to elucidate the background of that relation. With the objective to fill this gap and gain further understanding on the fundamental properties of ion conducting materials, we are studying systematically the mechanical properties of different materials. In the present study, after showing briefly our previous results obtained in crystalline materials, results regarding the relation between ionic conduction and mechanical properties in superionic glasses is presented. All these results indicate the intimate relation between the mechanical and ionic conduction. The results also indicate that the Grüneisen parameter and the Anderson–Grüneisen parameter of ionic conductors exhibit large temperature dependence and increase with temperature.

Keywords: ionic conductors; chalcogenide glasses; mechanical properties; elastic constants; elastic anisotropy; Grüneisen parameter; Anderson–Grüneisen parameter

Citation: Aniya, M.; Sadakuni, H.; Hirano, E. Ionic Conductors: Effect of Temperature on Conductivity and Mechanical Properties and Their Interrelations. *Crystals* **2021**, *11*, 1008.

https://doi.org/10.3390/cryst11081008

Academic Editor: Claudio Cazorla

Received: 27 July 2021
Accepted: 22 August 2021
Published: 23 August 2021

1. Introduction

The ionic transport and the mechanical properties in solids are intimately related. The existence of such relation is understandable, because, when an ion diffuses in a solid material it is accompanied by a local deformation of the medium, and reciprocally, the ion can be moved by deforming mechanically the ambient that surround the moving ion. Despite this fact, the number of studies done to elucidate the relation between the mechanical and other physical properties in ionic conductors are limited [1–33]. By searching the literature, we find diverse studies that are related with the subject in consideration. Some of them exbibit interesting but complex physical properties [6,12,23,24], whose mechanistic explanation are awaited. For instance, usually the sound velocity in solids decreases by increasing temperature. However, in β-Ag_3SI, a well-known ionic conductor, the sound velocity increases with temperature in the temperature interval between 157 K and 360 K [6]. Although the temperature range is limited, the increase of the sound velocity with temperature is also observed in the superionic phase of AgI [15]. To the best of our knowledge, no satisfactory explanation has been given to those observations. Interestingly, there have been reported that the thermal conductivity in β-Ag_3SI [34] and superionic AgI [35] increase with temperature. These behaviors are opposite to those observed usually. Theoretical study showed that such a behavior of thermal conductivity can be accounted for by the increase of hard-core like collision between the mobile ions and the surrounding lattice ions [36]. However, a different model is needed to understand the origin of the behavior obtained experimentally.

In recent years, much attention has been paid to heterostructures and interfaces to enhance the ionic conductivity [37–39]. At the interface region of the heterostructure, the mechanic stress is different from that in the bulk region. This difference originates the increase of the ionic mobility. On the other hand, studying the effect of multiple external

perturbances to ion dynamics is effective for the understanding of the mechanism of superionic conduction. For instance, light was used to study the influence of elastic stress on ionic transport in a heterojunction formed by a superionic crystal and an electrode [12]. The result provided a hint to understand the role of electrons in the ionic transport mechanism, a subject of fundamental importance but not thoroughly investigated [40–42]. Regarding this point, it will be enlightening to point out that the phenomenon reported in [12] has much in common with the photodoping effect known in the field of amorphous semiconductors [43–45]. Indeed, the mechanism of ionic conduction discussed in [12] is similar to that described in [44]. However, regarding the details on how the mechanical stress enters into the mechanism of light induced ionic transport remains to be solved. A related phenomena to that presented here is the acoustoionic and acoustoelectronic effect which has been investigated for many years [7,15]. By analyzing the data obtained there, we may extract useful information regarding the interaction between sound wave and charge carriers. The acoustoionic and acoustoelectronic interactions are manifested macroscopically in the sound velocity and attenuation. However, depending on the material in consideration and on the thermodynamic state, the observed phenomenon is quite complex. As an example, we may cite the behavior of internal friction reported in the superionic crystal Cu_6PS_5Br [23]. In this system, the effect of two different transitions, the superionic and ferroelastic transitions are reflected in the observed internal friction. Systematic investigation in these types of materials is expected to provide insights to understand the nature of interionic interactions of ionic conductors.

Understanding the mechanical properties of ionic conductors are also important from the application point of view [22,26,29,46–48]. From the side of materials synthesis, we may cite for instance, the mechanically milling process which are widely used in the preparation of solid electrolytes used in batteries [46]. The material properties that are gained from this method of synthesis depends on the mechanical properties of the materials. In recent years, much attention has been paid to develop all-solid-state lithium secondary batteries. To enhance the electrochemical performance of bulk-type batteries, an intimate solid–solid contact between electrode active materials and solid electrolytes is required in addition to high ionic conductivity [22]. It has been also recognized that the mechanical properties of the materials play a large role in the processing and assembly of batteries [26]. The mechanical strength of solid electrolytes plays an important role in suppressing the growth of dendrites, by increasing the interfacial stability and avoiding the propagation of cracks [47]. However, despite its importance, information on fundamental mechanical properties of battery materials is limited. A short summary of recent works on elastic, plastic, and fracture properties of crystalline oxide-based Li-ion solid electrolytes is available in [26]. As noted in many studies [22,26,29,46–48], the role of mechanical properties in a real battery system is multiple and complex. It extends from fundamental materials properties to assembly of devices.

With the objective to gain a further understanding on the fundamental properties of superionic materials, we are studying systematically the mechanical properties of different materials [17–20]. In the present report, after showing briefly the previous works done in our group, results regarding the relation between ionic conduction and elastic properties in superionic glasses will be presented. In particular, the results on temperature dependence of the Grüneisen and Anderson–Grüneisen parameters will be shown. Despite the fact that these quantities are intimately related with the anharmonicity of lattice vibrations, data of such quantities in ionic conductors are very scarce in the literature. Our study indicates that these quantities exhibit large temperature dependence and increase with the increase of temperature, results which are in accord with the ion transport properties, but not recognized throughout.

2. The Relation between Elastic Property and Ionic Conductivity

Usually, the elastic constants of the materials decrease by increasing temperature. It is known that the decrease is almost linear up to a temperature near to the melting

temperature. To see the peculiarity of ionic conductors, a comparison of the temperature dependence of the elastic constant C_{11} of ionic conductors and non-ionic conductors is shown in Figure 1 [49]. For the case of ionic conductors such as PbF_2 and BaF_2, the deviation from the linearity starts at a temperature much lower than the melting temperature. AgCl and AgBr are also compounds that exhibit relatively high ionic conductivity. For the case of AgCl, the deviation from the linearity is not so evident in Figure 1. However, it has been shown that its behavior contrasts with the behavior of typical ionic crystals, NaCl [19]. The other materials shown in Figure 1, Cu_2O, Al, and alkali halides are no ionic conductors.

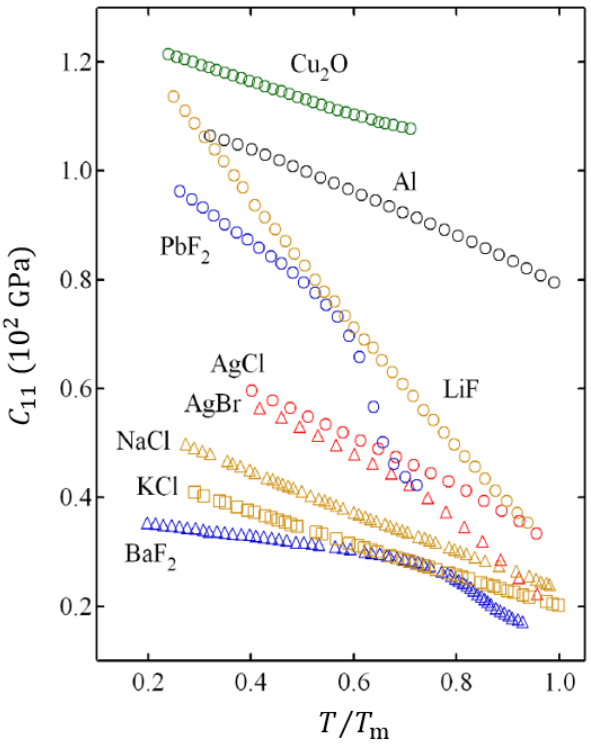

Figure 1. Temperature dependence of the elastic constant C_{11} of different materials [49]. The temperature is scaled by the melting temperature T_m.

The temperature dependence of the elastic constant arises from different factors. If we consider a crystal without defects, it arises from the variation of lattice potential energy associated with the anharmonicity. Therefore, the comparison of the temperature dependence of the elastic constants of different materials shown in Figure 1 provides a starting point to discuss the mechanical properties of ionic conductors.

The behavior shown in Figure 1 is related with the ionic transport properties of the materials, because crystal defects and lattice vibration anharmonicity are factors intimately related with the ionic conduction. This relation is seen more clearly in Figure 2, where the elastic constants and the ionic conductivity of PbF_2 are put in a single figure [17]. PbF_2 is one of the well-known superionic materials which exhibit a diffuse phase transition to the superionic state at T_c = 705 K. The figure shows clearly the correlation between the temperature dependencies of the ionic conductivity and the elastic constants. The ionic conductivity in PbF_2 starts to increase at around 600 K. At around the same temperature, the elastic constants start to deviate from the almost linear behavior observed at low temperature. At around 700 K, an abrupt increase of the ionic conductivity and large change in the elastic constants is discernible. The large increase of the ionic conductivity is commonly understood to arises from a development of extensive Frenkel disorder in the anion sublattice [50]. The behavior shown in Figure 2 suggests that the microscopic mechanisms that originate the mechanical and electrical properties have common elements. Indeed, in previous studies it has been shown that the elastic constants of ion conducting

materials AgCl and AgBr deviate from the linear behavior at high temperature, whereas the elastic constants of a typical ionic crystal NaCl retain their linearity up to a temperature close to the melting point [18,19]. Thus, we may say that the temperature dependence of the elastic constant provides much insight to understand ionic conductors.

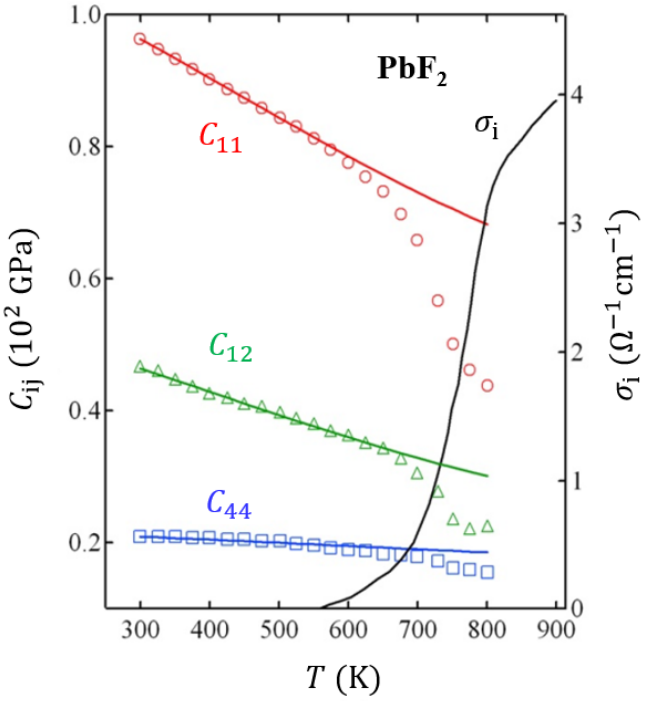

Figure 2. Temperature dependence of the elastic constants C_{ij} (C_{11}, C_{12} and C_{44}) and the ionic conductivity σ_i in PbF_2 [17].

The temperature dependence of the sound velocity in ionic conductors $CuGeAsS_3$ and $AgGeAsSe_3$ [11], show a behavior that supports the result shown in Figure 2. On the other hand, for the case of Cu_2Se, Cu_2Te, Ag_2Se and Ag_2Te, the temperature dependence of the Young's modulus, shear modulus and Poisson's ratio behave linearly, and no deviations or anomalies were detected at the superionic transition temperature [8]. The reason of this difference in the behavior is not clear. However, it will be useful to point out for a further study, that the transport properties of these chalcogenide materials depend on the details of chemical composition [51]. On the other hand, studies in the liquid phase of $Ag_{2+\delta}Se$ indicate that the sound velocity changes smoothly at the stoichiometric composition [52,53].

From Figure 2, we note that in PbF_2, the temperature dependence and the deviation from the linear behavior of C_{11} and C_{12} are much larger than that of C_{44}. Similar behavior has been also observed in other fluorite type ionic conductors such as CaF_2, SrF_2 and BaF_2 [54]. However, for these compounds, the degree of deviation from the linearity of C_{12} is comparable to that of C_{44}. An explanation to the different behavior of the temperature dependence of the elastic constants was given by arguing that C_{11} is determined from the contribution of Coulomb and short-range forces that have the same signs, whereas for C_{12} and C_{44} they have opposite signs, and that the effect of crystal defects on C_{12} and C_{44} cancel each other [4,54].

Similar behavior of the temperature dependence of elastic constants to that shown in Figure 2 has been also observed in AgCl and AgBr [10,13,16,18,19]. These crystals have the rock-salt structure. However, the physical properties of these compounds are different from the alkali halide compounds that have the same crystal structure. Particularly, the mechanical and ionic transport properties at high temperature are quite different. The silver halides exhibit a large increase of thermal expansion [55] and ionic conductivity [56] at high temperature. Therefore, we may argue that similar materials properties interrelation to that

shown in Figure 2 can be drawn. The peculiar behavior of AgCl and AgBr is considered to arise from a rapid increase in the concentration of Frenkel defects at high temperatures, which results from a temperature dependent decrease in the Gibbs free energy for defect formation [13,56]. Some authors suggest that the large softening of the elastic constants observed in silver halides is a manifestation of pre-melting phenomenon [56]. Others discuss that the temperature dependence of the elastic constants of AgCl and AgBr indicate the starting of the transition to the superionic state [13]. Such an interpretation seems consistent with a theoretical study on wave number dependent static dielectric function [57], which indicates that the superionic material in the liquid phase has a strong tendency to sublattice crystallization when compared to usual molten salts.

Among the elastic constants of AgCl and AgBr, C_{11} exhibits the largest temperature variation. The temperature dependence of C_{44} is small, and C_{12} exhibit an intermediate variation. In addition, AgBr exhibits a stronger deviation from the linearity than AgCl [10,13,16,18,19]. As discussed for the case of PbF_2, these observations indicate that specific force constants are more effectively interrelated with the atomic transport properties. This observation relates also with the different behavior of the Anderson–Grüneisen parameter discussed later.

The strong temperature dependence of the elastic constant of ionic conductors are usually interpreted to arise from the creation of large number of crystals defects [50,54,56]. On the other hand, it is also known that the elastic constants reflect the bonding nature of the materials [58]. In real situations, the plausible interpretation is that both factors and others if any, are reflected in the observed behavior. In the following, a result related with the bonding nature point of view is shown [19].

One of the quantities related with the directionality of the chemical bond is given by the Cauchy relation. For the case of cubic crystals, the Cauchy relation is given by $C_{12} = C_{44}$. If the interatomic interaction in a material consists only of radial interaction such as Coulomb interaction, the Cauchy relation is obeyed. In other words, by studying the deviation from the Cauchy relation, we can get information on the degree of non-radial interaction between the atoms. Figure 3 shows the temperature dependence of the ratio C_{44}/C_{12} in NaCl, AgCl and AgBr. Firstly, for the case of Ag halides we note a large deviation from $C_{44}/C_{12} = 1$, whereas NaCl starts to deviate from 1 at a temperature higher than 300 K. We also observe that C_{44}/C_{12} of Ag halides increase towards 1 with the increase of temperature. This temperature dependence is opposite to that observed in NaCl. It is worth mentioning at this point that the behavior shown in Figure 3 can be related with the bond fluctuation model of ion transport [40–42]. Although AgCl and AgBr have the rock-salt structure, their chemical bonding is not purely ionic as suggested from Figure 3. According to the bond fluctuation model, when an ion moves from one site to another site, it is accompanied by a local distortion of the electronic cloud that surrounds the mobile ion [40]. Since such distortions occur locally at different sites of the material and at different times, they can be visualized as local fluctuations of the chemical bond. The origin of the correlated ionic motions, which is a characteristic of superionic conductors is explained naturally from this model [40–42]. Results of ab-initio molecular dynamics study [59] and other recent studies support the view proposed in the bond fluctuation model [60–64]. From the point of view of this model, the result shown in Figure 3, in particularly the case of AgBr, suggests that the degree of central forces in the determination of elastic constants increases with the increase of temperature.

Regarding the temperature dependence of C_{44}/C_{12} in NaCl, a comment should be given. The behavior show in Figure 3 has been obtained by using the data reported in [65], where $C_{12} > C_{44}$. On the other hand, there are studies that report an opposite behavior, $C_{12} < C_{44}$ [66,67]. The difference in magnitude between C_{12} and C_{44} is not large, and in addition, the temperature variation of C_{12} is not monotonous [66,68]. Although small, its temperature derivative changes the sign from positive to negative at around 500 K [68]. As far as the authors are informed, there is no direct experimental study that judge which behavior is correct.

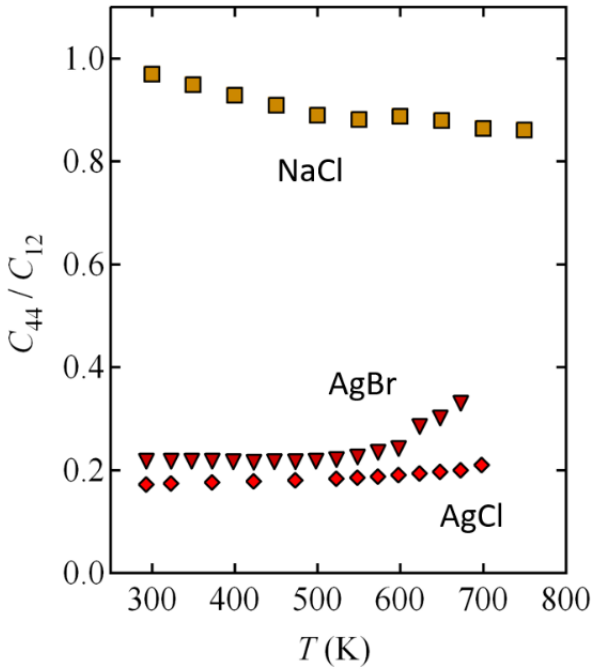

Figure 3. Temperature dependence of the ratio C_{44}/C_{12} in AgCl, AgBr and NaCl [18].

The elastic anisotropy influences a variety of physical phenomena. The results shown in Figures 2 and 3 suggest the possibility that the ionic conduction is related with the elastic anisotropy of the materials. This hypothesis has been investigated by applying an expression for the index of anisotropy [69] proposed some years ago.

$$A_U = \frac{6}{5}\left(\sqrt{A_Z} - \frac{1}{\sqrt{A_Z}}\right)^2, \tag{1}$$

where

$$A_Z = \frac{2C_{44}}{C_{11} - C_{12}}. \tag{2}$$

Here, A_Z is the so-called Zener's anisotropy, which is defined as the ratio between two quantities C_{44} and $(C_{11} - C_{12})/2$. The elastic constant C_{44}, represents the resistance to deformation with respect to a shear stress applied across the (100) plane in the [010] direction, whereas $(C_{11} - C_{12})/2$ represents the resistance to shear deformation applied across the (110) plane in the $[1\bar{1}0]$ direction. The expression of A_U given in Equation (1) has been introduced in such a way to give a single index of anisotropy, and its value is zero for an isotropic crystal [69].

Figure 4, shows the temperature dependence of A_U calculated for NaCl, AgCl and AgBr [18]. From the figure, we note that the A_U of AgBr exhibits very large temperature dependence. Particularly, we note that its elastic anisotropy starts to increase largely at around 550 K. For AgCl, its elastic anisotropy is larger al low temperature. It is also observed that AgCl and AgBr exhibit minimal values at around 600 K and 500 K, respectively. For the case of NaCl, the value of A_U and its temperature dependence is small. That is, NaCl is almost elastically isotropic over a wide temperature range. The result shown in Figure 4 suggests clearly that the elastic anisotropy is intimately related with the defect creation and the ionic conduction property of the materials. This is a new and interesting observation, because till very recently, no study on elastic anisotropy of solid electrolytes has been reported [29], excepting our preliminary study [18]. We are planning to extend the analysis of A_U to other ionic conducting materials to gain further information on this subject and draw a decisive conclusion.

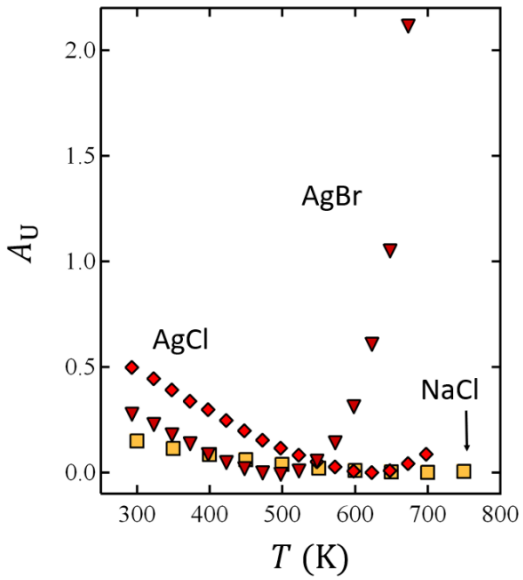

Figure 4. Temperature dependence of the anisotropy index A_U in NaCl, AgCl and AgBr [18].

3. Temperature Dependence of the Anderson–Grüneisen Parameter

An understanding of the anharmonic effects and the temperature dependent thermo-mechanical properties is of primordial importance in ionic conducting materials. In Figure 1, it was shown that the elastic constants vary linearly at low temperatures. Such behavior is described by a temperature independent Anderson–Grüneisen (AG) parameter which is given by [70]:

$$\delta = -\frac{1}{\alpha B_T}\left(\frac{\partial B_T}{\partial T}\right)_P = -\frac{V}{B_T}\left(\frac{\partial B_T}{\partial V}\right)_P, \quad (3)$$

where α is the thermal expansion coefficient, B_T is the isothermal bulk modulus, V is the volume, T is the temperature, and P is the pressure. The AG parameter has been introduced as an attempt to improve the description of the temperature dependent Young's modulus [70]. Nowadays, it is used as an important tool for investigating different aspects related to thermoelastic properties of solids. Although there are some studies reporting its temperature dependence [20], usually, the AG parameter is considered as a constant of the material or depends only weakly on temperature [71]. However, for the case of ionic conducting materials, we have found that the AG parameter depends strongly on temperature [20].

The result shown in Figure 5 indicates clearly the difference between the behavior of ion conducting materials AgCl, AgBr and CaF_2 and the other non-ion conducting materials KBr, Mg_2SiO_2 and Ag. For the cases of AgBr and CaF_2 we observe a peak. Such kind of peaked behavior has been also observed in other ionic conducting materials investigated, PbF_2 and BaF_2 [20]. The peak of the AG parameter at certain temperature arises from the different relative contributions of temperature derivatives of C_{11}, C_{12} and the thermal expansion coefficient. For instance, for the case of fluorine compounds investigated, it was discussed that when the temperature dependence of C_{11} dominates, the AG curve shows an upward curvature, whereas when the temperature dependences of C_{12} and thermal expansion coefficient dominate, the AG curve shows a downward curvature. On the other hand, the peak of AG parameter observed in AgBr arises mainly from the thermal expansion coefficient which exhibit a large temperature dependence. Indeed, if the temperature dependence of the thermal expansion coefficient is ignored, the peaked behavior is not observed [20]. The result of the analysis mentioned, points that the increase of the anharmonicity which is quantified by the AG parameter has different components.

In other words, although the different materials parameters are interrelated, the analysis provides a hint to design a material with enhanced ionic conductivity.

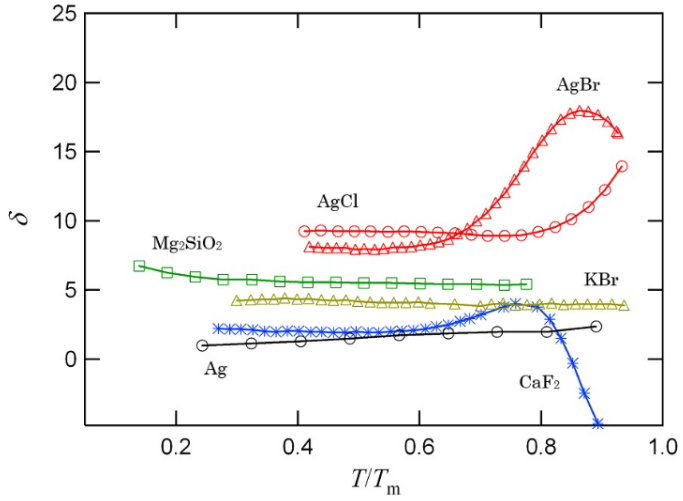

Figure 5. The Anderson–Grüneisen parameter δ of some materials as a function of normalized temperature T/T_{m}, where T_{m} is the melting temperature.

In a previous section, it was pointed out that not all the elastic constants exhibit the same temperature dependence. This observation is also reflected in the behavior of the Anderson–Grüneisen parameter. An example is shown in Figure 6 for the case of ion conducting material AgBr. We note that δ_{11} and δ_{12} that are associated with C_{11} and C_{12} exhibit strong temperature dependence. On the other hand, the temperature dependence of δ_{44} associated with C_{44} is weak. The result indicates again that C_{11} and C_{12}. are more deeply involved than C_{44} in the appearance of the ionic conductivity. Since the elastic constants C_{ij} can be understood in principle from the interatomic interaction point of view, the result provides an important clue to understand the microscopic mechanism of ion transport. For instance, in a previous report [20] it was pointed out that the scaled value of $\delta_{11}(T_{\mathrm{R}})/\delta_{11}(300\ \mathrm{K}) = 1.2$ correlates with the value of Frenkel defect formation energy at temperature T_{R}.

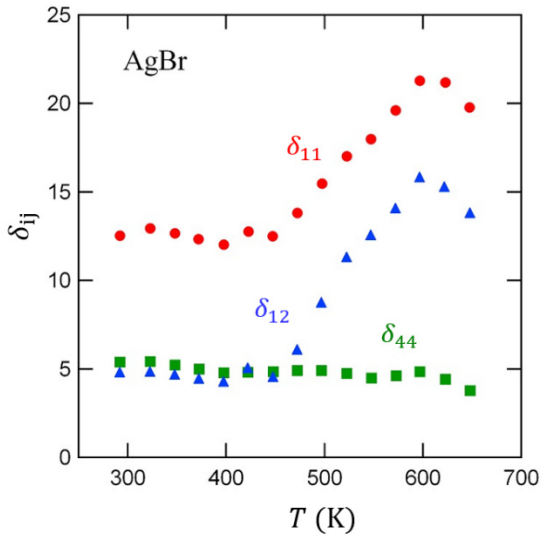

Figure 6. Temperature dependence of the mode Anderson–Grüneisen parameter δ_{ij} of AgBr [18].

The results shown above were focused on temperature dependence of elastic constants. As pointed elsewhere [40], the crystalline ionic conductors exhibit a structural phase

transformation under the action of relatively low pressure. Experimental studies confirm this conjecture [63,72]. A reason for this behavior resides in the weak angular force constant that the ionic conducting materials have. For the case of zinc-blend structure compounds, the elastic constants can be written in terms of bond stretching and bond bending force constants and Coulombic forces [73,74]. Typical ionic conductors such as γ-AgI and Cu halides have the zinc-blend type structure. The pressure dependence of the force constant of CuCl, CuBr and CuI indicated that the bond stretching force constant increases, whereas the bond bending force constant decreases with the increase of pressure [75]. These studies suggest that weakening of angular force constant is favorable for the ionic conduction. However, it is important to recognize that a complete absence of angular force constant is not favorable for ionic conduction. For the promotion of a correlated ionic motion, the presence of certain degree of angular force is indispensable. The bond fluctuation model mentioned above [40–42] provides the physical background to the discussion given here.

4. Grüneisen Parameter and Ionic Conductivity in Glasses

In conjunction with the AG parameter mentioned above, the Grüneisen parameter which describes the relationship between phonon frequency and volume, is a quantity widely used in the discussion of anharmonic lattice vibrations. The Grüneisen equation of state which includes the Grüneisen parameter is considered as one of the most valuable thermodynamic equation of state [76,77], because it links the phonon energy to the potential energy of the material. In the thermodynamic description, the Grüneisen parameter is written as:

$$\gamma = \frac{\alpha B_T V}{C_V}, \tag{4}$$

where α is the thermal expansion coefficient, B_T is the isothermal bulk modulus, V is the molar volume, and C_V is the molar heat capacity. Despite their importance, data of δ and γ in ionic conducting materials are quite limited [18,20,42,78–83]. In view of this situation, we started a program to evaluate the Grüneisen parameter of ionic conductors. However, for the evaluation of γ we need to know the values of various quantities appearing in Equation (4), which is not easy to find. Therefore, developing a different way of evaluation is highly desirable. Some years ago, a method of evaluation of γ that uses only the sound velocity was proposed [84]. According to that work, the Grüneisen parameter is given by:

$$\gamma = \frac{3}{2}\left[\frac{3(V_L/V_T)^2 - 4}{(V_L/V_T)^2 + 2}\right], \tag{5}$$

where V_L and V_T are the longitudinal and transverse sound velocities, respectively. It has been shown that the evaluation based on Equation (5) shows a satisfactory agreement with the evaluation based on Grüneisen equation [84]. The expression given in Equation (5) is convenient in the analysis of mechanical properties of glassy materials, because for isotropic materials the sound velocities can be written as:

$$V_L = \left(\frac{B_T + 4G/3}{\rho}\right)^{1/2}, \tag{6}$$

and

$$V_T = \left(\frac{G}{\rho}\right)^{1/2}, \tag{7}$$

where B_T, G and ρ are the bulk modulus, shear modulus and density, respectively.

Figure 7 shows the temperature dependence of the Grüneisen parameter γ of ion conducting glasses $x$$Ag_2S$-$(1-x)$$AgPO_3$. We note that the Grüneisen parameter increases with the increase of temperature. As in the case of AG parameter mentioned above, usually, the Grüneisen parameter is considered as a constant or weakly temperature dependent quantity [77]. This type of behavior is illustrated in Figure 8, for the case of chalcogenide

glasses that are not ionic conductors. The values of γ shown in Figures 7 and 8 were evaluated from sound velocity data reported in [81,85], following Equation (5). The comparison between the behavior shown in Figures 7 and 8 shows clearly the difference between the γ of ion-conducting and non-ion-conducting glasses.

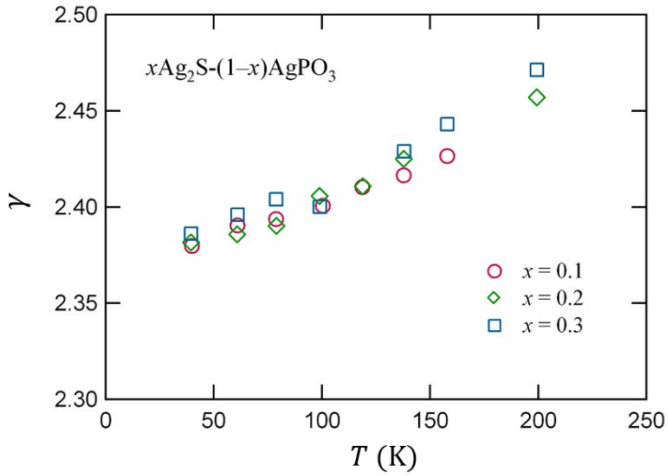

Figure 7. Temperature dependence of the Grüneisen parameter of xAg$_2$S-(1 − x) AgPO$_3$ glasses.

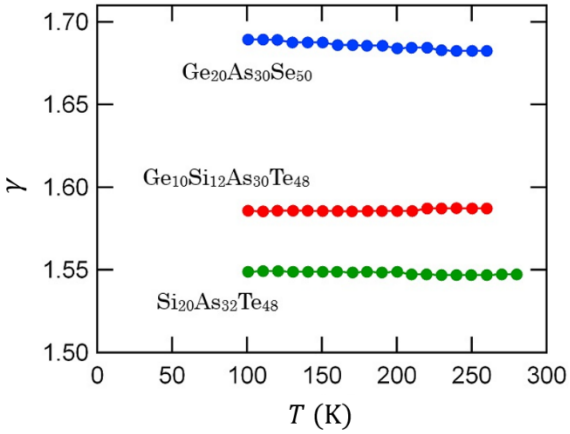

Figure 8. Temperature dependence of the Grüneisen parameter of $Ge_{20}As_{30}Se_{50}$, $Ge_{10}Si_{12}As_{30}Te_{48}$, and $Si_{20}As_{32}Te_{48}$ glasses.

The glassy systems can be considered to consist from an agglomeration of structural units. On the other hand, as can be inferred from the discussion given in previous sections, the Grüneisen parameter of glassy materials contains information on the softness of the connectivity between the structural units. From this point of view, the result shown in Figure 8 indicates that the connectivity remains almost the same in the temperature range shown. On the other hand, the result shown in Figure 7 indicates that the connectivity varies largely with temperature. This way of understanding is in line with a recent model for the viscosity of glass forming liquids [86,87]. There, the viscous flow and the structural relaxation are considered to result from thermally activated bond-breaking and bond-switching processes. According to this model, the temperature dependence of the viscosity is described by the mean values of the bond strength and the coordination number, and their fluctuations of the structural units that form the melt. Within this model, it is envisaged that in ion conducting glassy materials, the fluctuation between the structural units plays an important role. Recently, some studies regarding the interrelation between the mechanical properties and ionic conductivity in mixed network former glasses [30] and gel polymer

electrolytes [31] have been reported. It will be interesting to investigate if the model mentioned above [86,87] conforms with the experimental findings reported in [30,31].

In view of the result shown in Figure 2, and the discussion given above, it is of considerable interest to investigate the relation between the Grüneisen parameter and the ionic conductivity. A result for the case of xAg$_2$S-(1 − x)AgPO$_3$ glasses is shown in Figure 9. Here, the ionic conductivities corresponding to low temperatures were evaluated by extrapolating the data reported in [88,89]. As expected, we observe that the ionic conductivity increases with the value of γ. As mentioned above, the observed behavior can be understood to arise from the weakening of the connectivity between the structural units that form the glass by increasing the temperature. However, it does not imply that a structural unit moves as whole. The structural unit forms a network and the ion that breaks the local constraint originates the ionic conduction. That is, the ionic conductivity results from the decoupling between the network and the mobile ions [86,87,90,91].

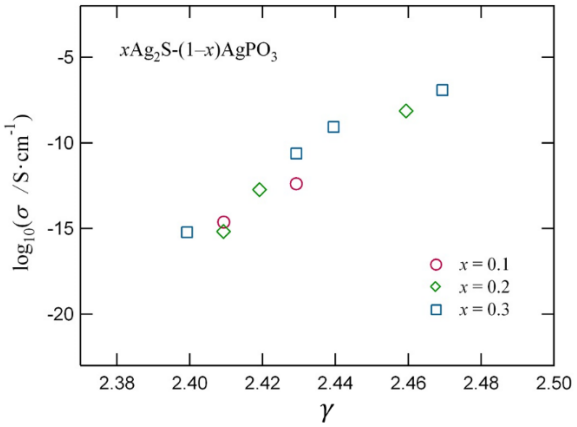

Figure 9. Relation between the Grüneisen parameter and the ionic conductivity in xAg$_2$S-(1 − x) AgPO$_3$ glasses.

In this report we have focused in to show how the AG parameter and the Grüneisen parameter of glassy materials are related with the ionic conduction. The elastic properties of glasses such as the Young's modulus and Poisson's ratio allows to get insight into the short and medium range orders existing in glasses [92]. Regarding the role of medium range structure on ionic transport, it has been shown that in AgI-containing superionic glasses, the activation energy of ion transport decreases with the decreases in the wave number of first-sharp-diffraction-peak (FSDP) [93]. The FSDP reflects the presence of an intermediate range ordering within the glass.

5. Conclusions

In the present report, it was shown that the temperature dependence of the elastic constants in ionic conductors are intimately related with the temperature dependence of the ionic conductivity. The analysis of the temperature dependence of elastic constants reveals that in cubic materials such as PbF_2 and AgBr, the force constants associated with C_{11} and C_{12} are related strongly with the atomic transport properties. It was also shown that the elastic anisotropy is intimately related with the defect creation and ionic transport property of the materials. Data of Grüneisen and Anderson–Grüneisen parameters were presented. Despite these quantities reflect the degree of anharmonicity of lattice vibrations, they are rarely reported in the literature. Our result indicates that in ion conducting materials, the temperature dependence of the Grüneisen and Anderson–Grüneisen parameters are large. Result in ion conducting glasses revealed that the ionic conductivity increases with the increase of Grüneisen parameter. All these observations indicate that studies of mechanical properties provide much insight to understand the materials properties of ionic conductors. However, for its deep understanding further studies on diverse materials is necessary. In the present report, we have concentrated in to present results on

prototypical ionic conductors. Nowadays, many new ionic conductors having complex chemical compositions and crystallographic structures have been synthesized. We expect that the present study could serve as a basis to understand the mechanical properties of these new materials.

Author Contributions: Conceptualization, M.A.; methodology, M.A. and H.S.; validation, H.S. and E.H.; formal analysis, H.S. and E.H.; investigation, H.S., E.H. and M.A.; data curation, H.S. and E.H.; writing—original draft preparation, M.A.; writing—review and editing, M.A.; visualization, H.S. and E.H.; supervision, M.A.; project administration, M.A.; funding acquisition, M.A. All authors have read and agreed to the published version of the manuscript.

Funding: This work was funded in part by JST CREST, Japan, No. JPMJCR1861 and No. JPMJCR18I2, and by JSPS KAKENHI No. 20K05080, No. 20H02430 and No. 21K04660.

Conflicts of Interest: The authors declare no conflict of interest.

References

1. Fjeldly, T.A.; Hanson, R.C. Elastic and piezoelectric constants of silver-iodide: Study of a material at the covalent-ionic phase transition. *Phys. Rev. B* **1974**, *10*, 3569–3577. [CrossRef]
2. Hattori, T.; Imanishi, T.; Kurokawa, H.; Mitsuishi, A. Brillouin scattering in silver halides. *J. Physique* **1981**, *42*, C6-920. [CrossRef]
3. Aliev, A.E.; Fershtat, L.N.; Khabibullaev, P.K. Acoustic anomalies in lanthanum trifluoride in the region of the phase transitions in the superionic state. *High Temp.* **1984**, *22*, 381–385.
4. Masasreh, M.O.; Pederson, D.O. Elastic constants of cubic lead fluoride from 300 to 850 K. *Phys. Rev. B* **1984**, *30*, 3482–3485. [CrossRef]
5. Carini, G.; Cutroni, M.; Federico, M.; Galli, G.; Tripodo, G. Acoustic properties and diffusion in superionic glasses. *Phys. Rev. B* **1984**, *30*, 7219–7224. [CrossRef]
6. Kanashiro, T.; Michihiro, Y.; Ozaki, J.; Ohno, T.; Kojima, A. Ultrasonic measurements in the ionic conductor β-Ag_3SI. *J. Phys. Soc. Jpn.* **1987**, *56*, 560–564. [CrossRef]
7. Kezhionis, A.; Samulionis, V.; Skritskij, V.; Ukshe, E.A. Ultrasonic investigation of phase transition and relaxational phenomena in superionic NASICON. *Solid State Ion.* **1989**, *36*, 235–238. [CrossRef]
8. Berezin, V.M.; Pashnin, M.I. Temperature dependence of the elastic moduli of copper and silver chalcogenides. *Sov. Phys. Solid State* **1992**, *34*, 162–163.
9. Manasreh, M.O.; Pederson, D.O. Elastic constants of barium fluoride from 300 to 1250 K. *Phys. Rev. B* **1985**, *31*, 3960–3964. [CrossRef] [PubMed]
10. Hughes, W.C.; Cain, L.S. Second-order elastic constants of AgCl from 20 to 430 °C. *Phys. Rev. B* **1996**, *53*, 5174–5180. [CrossRef]
11. Gorin, Y.F.; Mel'nikova, N.V.; Baranova, E.R.; Kobeleva, O.L. Influence of ionic conductivity on the elastic characteristics of four-component copper and silver chalcogenides. *Tech. Phys. Lett.* **1997**, *23*, 550–552. [CrossRef]
12. Bredikhin, S.I.; Bogatyrenko, M.V. The influence of elastic stress fields on ionic transport through a (superionic crystal)–(electrode) heterojunction. *Phys. Solid State* **1999**, *41*, 1620–1625. [CrossRef]
13. Cain, L.S.; Hu, G. High-temperature elastic constants of AgBr. *Phys. Rev. B* **2001**, *64*, 104104. [CrossRef]
14. Reddy, C.N.; Chakradhar, R.P.S. Elastic properties and spectroscopic studies of fast ion conducting Li_2O-ZnO-B_2O_3 glass system. *Mater Res. Bull.* **2007**, *42*, 1337–1347. [CrossRef]
15. Samulionis, V.; Jonkus, V. Investigation of acoustoionic and acoustoelectronic interaction in fast ionic conductors. *Solid State Ion.* **2008**, *179*, 120–125. [CrossRef]
16. Endou, S.; Michihiro, Y.; Itsuki, K.; Nakamura, K.; Ohno, T. RUS study of the elastic constants in silver halide crystals. *Solid State Ion.* **2009**, *180*, 488–491. [CrossRef]
17. Sadakuni, H.; Aniya, M. Analysis of temperature dependence of the second-order elastic constants of PbF_2. *Phys. Rep. Kumamoto Univ.* **2012**, *14*, 15–20.
18. Sadakuni, H.; Aniya, M. Temperature dependence of elastic parameters of ionic conductors. In *Solid State Ionics, Ionics for Sustainable World*; Chowdari, B.V.R., Kawamura, J., Mizusaki, J., Amezawa, K., Eds.; World Scientific: Singapore, 2012; pp. 705–713, ISBN 978-981-4415-03-3.
19. Aniya, M.; Sadakuni, H. Analysis of the temperature dependence of elastic constants of AgCl. *Thermochim. Acta* **2012**, *532*, 111–114. [CrossRef]
20. Sadakuni, H.; Aniya, M. Anomalous temperature dependency of the Anderson-Grüneisen parameters in high ionic conductors. *Phys. B* **2013**, *410*, 81–84. [CrossRef]
21. Yadawa, P.K. Non-destructive characterization of superionic conductor: Lithium nitride. *Mater. Sci. Poland* **2014**, *32*, 626–632. [CrossRef]
22. Kato, A.; Nagao, M.; Sakuda, A.; Hayashi, A.; Tatsumisago, M. Evaluation of Young's modulus of Li_2S-P_2S_5-P_2O_5 oxysulfide glass solid electrolytes. *J. Ceram. Soc. Jpn.* **2014**, *122*, 552–555. [CrossRef]

23. Bilanych, V.S.; Buchuk, R.Y.; Petrachenkov, A.E.; Skubenych, K.V.; Studenyak, I.P. Internal Friction in Cu_6PS_5Br superionic crystals and related composites. *Phys. Solid State* **2014**, *56*, 739–745. [CrossRef]
24. Ismail, M.; Supardan, S.N.; Yahya, A.K.; Yusof, M.I.M.; Halimah, M.K. Anomalous elastic and optical behaviours of mixed electronic-ionic of $x$$Ag_2O$-$(35-x)$[$0.5MoO_3$-$0.5V_2O_5$]-$65TeO_2$ conductor glasses. *Chalc. Lett.* **2016**, *13*, 489–505.
25. Cheng, E.J.; Taylor, N.J.; Wolfenstine, J.; Sakamoto, J. Elastic properties of lithium cobalt oxide ($LiCoO_2$). *J. Asian Ceram. Soc.* **2017**, *5*, 113–117. [CrossRef]
26. Wolfenstine, J.; Allen, J.L.; Sakamoto, J.; Siegel, D.J.; Choe, H. Mechanical behavior of Li-ion-conducting crystalline oxide-based solid electrolytes: A brief review. *Ionics* **2018**, *24*, 1271–1276. [CrossRef]
27. Bilanich, V.S.; Skubenych, K.V.; Babilya, M.I.; Pogodin, A.I.; Studenyak, I.P. The effect of isovalent cation substitution on mechanical properties of $(Cu_xAg_{1-x})_7SiS_5I$ superionic mixed single crystals. *Ukr. J. Phys.* **2020**, *65*, 453–457. [CrossRef]
28. Garcia-Mendez, R.; Smith, J.G.; Neuefeind, J.C.; Siegel, D.J.; Sakamoto, J. Correlating macro and atomic structure with elastic properties and ionic transport of glassy Li_2S-P_2S_5 (LPS) solid electrolyte for solid-state Li metal batteries. *Adv. Energy Mater.* **2020**, *10*, 2000335. [CrossRef]
29. Ke, X.; Wang, Y.; Ren, G.; Yuan, C. Towards rational mechanical design of inorganic solid electrolytes for all-solid-state lithium ion batteries. *Energy Storage Mater.* **2020**, *26*, 313–324. [CrossRef]
30. Wang, W.; Christensen, R.; Curtis, B.; Martin, S.W.; Kieffer, J. A new model linking elastic properties and ionic conductivity of mixed network former glasses. *Phys. Chem. Chem. Phys.* **2020**, *20*, 1629–1641. [CrossRef]
31. Zhang, X.; Liu, S.; Zheng, Y.; Koh, X.; Lim, Q.F.; Sharma, M.; Fam, D.W.H. Elucidating the relationship between mechanical properties and ionic conductivity in a highly conductive gel polymer electrolyte. *Mater. Lett.* **2021**, *294*, 129789. [CrossRef]
32. Baktash, A.; Demir, B.; Yuan, Q.; Searles, D.J. Effect of defects and defect distribution on Li-diffusion and elastic properties of anti-perovskite Li_3OCl solid electrolyte. *Energy Storage Mater.* **2021**, *41*, 614–622. [CrossRef]
33. Iguchi, F.; Hinata, K. High-temperature elastic properties of yttrium-doped barium zirconate. *Metals* **2021**, *11*, 968. [CrossRef]
34. Saito, F.; Tozaki, K.; Kojoma, A. Thermal conductivity of superionic conductor Ag_3SI. *J. Phys. Soc. Jpn.* **1993**, *62*, 3351–3352. [CrossRef]
35. Goetz, M.C.; Cowen, J.A. The thermal conductivity of silver iodide. *Solid State Commun.* **1982**, *41*, 293–295. [CrossRef]
36. Aniya, M.; Usuki, T.; Kobayashi, M.; Okazaki, H. Liquidlike model for thermal conductivity in superionic conductors. *Phys. Rev. B* **1990**, *41*, 7113–7117. [CrossRef] [PubMed]
37. Aniya, M. A note on the possibility of conductivity enhancement in fast ion conductor superlattices. *Jpn. J. Appl. Phys.* **1990**, *29*, 67–68. [CrossRef]
38. Sata, N.; Eberman, K.; Eberl, K.; Maier, J. Mesoscopic fast ion conduction in nanometre-scale planar heterostructures. *Nature* **2000**, *408*, 946–949. [CrossRef]
39. Lee, D.; Gao, X.; Sun, L.; Jee, Y.; Poplawsky, J.; Farmer, T.O.; Fan, L.; Guo, E.-J.; Lu, Q.; Heller, W.T.; et al. Colossal oxygen vacancy formation at a fluorite-bixbyite interface. *Nat. Commun.* **2020**, *11*, 1371. [CrossRef]
40. Aniya, M. A chemical approach for the microscopic mechanism of fast ion transport in solids. *Solid State Ion.* **1992**, *50*, 125–129. [CrossRef]
41. Aniya, M. Bond fluctuation model of superionic conductors: Concepts and applications. *Integr. Ferroelec.* **2010**, *115*, 81–94. [CrossRef]
42. Aniya, M. Bonding character and ionic conduction in solid electrolytes. *Pure Appl. Chem.* **2019**, *91*, 1797–1806. [CrossRef]
43. Kolobov, A.V.; Elliott, S.R. Photodoping of amorphous chalcogenides by metals. *Adv. Phys.* **1991**, *40*, 625–684. [CrossRef]
44. Aniya, M. A model for the photo-electro ionic phenomena in chalcogenide glasses. *J. Non-Cryst. Solids* **1996**, *198–200*, 762–765. [CrossRef]
45. Sakaguchi, Y.; Hanashima, T.; Simon, A.-A.A.; Mitkova, M. Silver photodiffusion into amorphous Ge chalcogenides. *Eur. Phys. J. Appl. Phys.* **2020**, *90*, 30101. [CrossRef]
46. Li, X.; Liang, J.; Yang, X.; Adair, K.R.; Wang, C.; Zhao, F.; Sun, X. Progress and perspectives on halide lithium conductors for all-solid -state lithium batteries. *Energy Environ. Sci.* **2020**, *13*, 1429–1461. [CrossRef]
47. Yang, X.; Adair, K.R.; Gao, X.; Sun, X. Recent advances and perspectives on thin electrolytes for high-energy-density solid-state lithium batteries. *Energy Environ. Sci.* **2021**, *14*, 643–671. [CrossRef]
48. Agarkova, E.A.; Zadorozhnaya, O.Y.; Burmistrov, I.N.; Yalovenko, D.V.; Agaekov, D.A.; Rabotkin, S.V.; Solovyev, A.A.; Nepochatov, Y.K.; Levin, M.N.; Bredikhin, S.I. Relationships between mechanical stability of the anode supports and electrochemical performance of intermediate-temperature SOFCs. *Mater. Lett.* **2021**, *303*, 130516. [CrossRef]
49. Sadakuni, H. Study of Elastic Properties of Ionic Conductors. Ph.D. Thesis, Kumamoto University, Kumamoto, Japan, 25 March 2013.
50. Oberschmidt, J. Effect of Frenkel defects on the high-pressure phase transitions in PbF_2 and $SrCl_2$. *Phys. Rev. B* **1981**, *24*, 3584–3587. [CrossRef]
51. Sitte, W. Chemical diffusion in mixed conductors: α'-Ag_2Te and β-Ag_2Se. *Solid State Ion.* **1997**, *94*, 85–90. [CrossRef]
52. Tsuchiya, Y. Velocity of sound and high-energy γ-ray attenuation in liquid Ag-Se alloys. *J. Phys. Condens. Matter.* **1996**, *8*, 1897. [CrossRef]
53. Aniya, M.; Iseki, T. A model for the composition dependence of sound velocity in liquid silver chalcogenides. *J. Non-Cryst. Solids* **2002**, *312–314*, 400–403. [CrossRef]

54. Catlow, C.R.A.; Comins, J.D.; Germano, F.A.; Harley, R.T.; Hayes, E. Brillouin scattering and theoretical studies of high-temperature disorder in fluorite crystals. *J. Phys. C Solid State Phys.* **1978**, *11*, 3197–3212. [CrossRef]
55. Lawn, B.R. Thermal expansion of silver halides. *Acta Cryst.* **1963**, *16*, 1163–1169. [CrossRef]
56. Aboagye, J.K.; Friauf, R.J. Anomalous high-temperature ionic conductivity in the silver halides. *Phys. Rev. B* **1975**, *11*, 1654–1664. [CrossRef]
57. Aniya, M.; Okazaki, H.; Kobayashi, M. Static dielectric function of superionic conductor α-AgI. *Phys. Rev. Lett.* **1990**, *65*, 1474, Erratum: *Phys. Rev. Lett.* **1990**, *65*, 2920. [CrossRef] [PubMed]
58. Harrison, W. *Electronic Structure and the Properties of Solids*; W.H. Freeman and Company: San Francisco, CA, USA, 1980; ISBN 0-486-66021-4.
59. Shimojo, F.; Aniya, M. Diffusion of mobile ions and bond fluctuations in superionic conductor CuI from ab initio molecular-dynamics simulations. *J. Phys. Soc. Jpn.* **2003**, *72*, 2702–2705. [CrossRef]
60. Adelstein, N.; Wood, B.C. Role of dynamically frustrated bond disorder in a Li^+ superionic solid electrolyte. *Chem. Mater.* **2016**, *28*, 7218–7231. [CrossRef]
61. Düel, A.; Heitjans, P.; Fedorov, P.; Scholz, G.; Cibin, G.; Chadwick, A.V.; Pickup, D.M.; Ramos, S.; Sayle, L.W.L.; Sayle, E.K.L.; et al. Is geometric frustration-induced disorder a recipe for high ionic conductivity? *J. Am. Chem. Soc.* **2017**, *139*, 5842–5848. [CrossRef]
62. Kweon, K.E.; Varley, J.B.; Shea, P.; Adelstein, N.; Mehta, P.; Heo, T.W.; Udovic, T.J.; Stavila, V.; Wood, B.C. Structural, chemical, and dynamical frustration: Origins of superionic conductivity in closo-borate solid electrolytes. *Chem. Mater.* **2017**, *29*, 9142–9153. [CrossRef]
63. Moury, R.; Łodziana, Z.; Remhof, A.; Duchêne, L.; Roedern, E.; Gigante, A.; Hagemann, H. Pressure-induced phase transitions in $Na_2B_{12}H_{12}$, structural investigation on a candidate for solid-state electrolyte. *Acta Cryst. B* **2019**, *75*, 406–413. [CrossRef]
64. Abudouwufu, T.; Zuo, W.; Palenovich, V.; Zhang, X.; Zeng, X.; Tolstoguzov, A.; Zou, C.; Tian, C.; Fu, D. Crystal structure and ion transport properties of solid electrolyte $CsAg_4Br_{3-x}I_{2+x}$ ($0 < x < 1$). *Solid State Ion.* **2021**, *364*, 115634. [CrossRef]
65. Liu, Q.; He, Q. Elastic constants for various classes of solids at high temperature. *Acta Phys. Pol. A* **2007**, *112*, 69–76. [CrossRef]
66. Slagle, O.D.; McKinstry, H.A. Temperature dependence of the elastic constants of the alkali halides. I. NaCl, KCl, and KBr. *J. Appl. Phys.* **1967**, *38*, 437–446. [CrossRef]
67. Vijay, A.; Verma, T.S. Analysis of temperature dependence of elastic constants and bulk modulus for ionic solids. *Phys. B* **2000**, *291*, 373–378. [CrossRef]
68. Yamamoto, S.; Ohno, I.; Anderson, O.L. High temperature elasticity of sodium chloride. *J. Phys. Chem. Solids* **1987**, *48*, 143–151. [CrossRef]
69. Ranganathan, S.I.; Ostoja-Starzewski, M. Universal elastic anisotropy index. *Phys. Rev. Lett.* **2008**, *101*, 055504. [CrossRef] [PubMed]
70. Anderson, O.L. Derivation of Wachtman's equation for the temperature dependence of elastic moduli of oxide compounds. *Phys. Rev.* **1966**, *144*, 553–557. [CrossRef]
71. Pandey, V.; Gupta, S.; Tomar, D.S.; Goyal, S.C. Analysis of Anderson- Grüneisen parameter under high temperature in alkaline earth oxides. *Phys. B* **2010**, 4943–4947. [CrossRef]
72. Hull, S. Superionics: Crystal structures and conduction processes. *Rep. Prog. Phys.* **2004**, *67*, 1233–1314. [CrossRef]
73. Martin, R.M. Elastic properties of ZnS structure semiconductors. *Phys. Rev. B* **1970**, *1*, 4005–4011. [CrossRef]
74. Lucovsky, G.; Martin, R.M.; Burstein, E. Localized effective charges in diamond crystals. *Phys. Rev. B* **1971**, *4*, 1367–1374. [CrossRef]
75. Aniya, M. Interatomic force constants and localized effective charges in copper halides. *Solid State Ion.* **1999**, *121*, 281–284. [CrossRef]
76. Zhang, X.; Sun, S.; Xu, T.; Zhang, T.Y. Temperature dependent Grüneisen parameter. *Sci. China Tech. Sci.* **2019**, *62*, 1565–1576. [CrossRef]
77. Drebushchak, V.A. Thermal expansion of solids: Review on theories. *J. Therm. Anal. Cal.* **2020**, *142*, 1097–1113. [CrossRef]
78. Ruppin, R. Grüneisen parameters of CaF_2 and BaF_2 from a lattice dynamical shell model. *J. Phys. Chem. Solids* **1972**, *33*, 83–86. [CrossRef]
79. Bogue, R.; Sladek, R.J. Elasticity and thermal expansivity of $(AgI)_x(AgPO_3)_{1-x}$ glasses. *Phys. Rev. B* **1990**, *42*, 5280–5288. [CrossRef] [PubMed]
80. Murin, I.V.; Glumov, O.V.; Gunβer, W. High pressure studies of superionic conductors with predominant anionic conductivity. *Ionics* **1995**, *1*, 274–278. [CrossRef]
81. Saunders, G.A.; Metcalfe, R.D.; Cutroni, M.; Federico., M.; Piccolo, A. Elastic and anelastic properties, vibrational anharmonicity, and fractal bond connectivity of superionic glasses. *Phys. Rev. B* **1996**, *53*, 5287–5300. [CrossRef]
82. Carini, G.; Carini, G.; D'Angelo, G.; Tripodo, G.; Bartolotta, A.; Salvato, G. Ultrasonic relaxations, anharmonicity, and fragility in lithium borate glasses. *Phys. Rev. B* **2005**, *72*, 014201. [CrossRef]
83. Dologlou, E. The role of Anderson-Gruneisen parameter in the estimation of self-diffusion coefficients in alkaline earth oxides. *J. Appl. Phys.* **2012**, *11*, 096101. [CrossRef]
84. Sanditov, D.S.; Mantatov, V.V.; Sanditov, B.D. Anharmonicity of lattice vibrations and transverse deformation of crystalline and vitreous solids. *Phys. Solid State* **2009**, *51*, 998–1003. [CrossRef]

85. Farley, J.M.; Saunders, G.A. Ultrasonic wave velocities and attenuation in IVb-Vb-VIb chalcogenide glasses: 2–300 K. *J. Non-Cryst. Solids* **1975**, *18*, 417–427. [CrossRef]
86. Aniya, M.; Ikeda, M. The bond strength-coordination number fluctuation model of viscosity: Concept and applications. *J. Polym. Res.* **2020**, *27*, 165. [CrossRef]
87. Aniya, M.; Ikeda, M. Arrhenius crossover phenomena and ionic conductivity in ionic glass-forming liquids. *Phys. Status Solidi B* **2020**, *257*, 2000139. [CrossRef]
88. Baud, G.; Besse, J.P. Superionic conducting glasses: Glass formation and conductivity in the system Ag_2S-$AgPO_3$. *J. Am. Ceram. Soc.* **1981**, *64*, 242–244. [CrossRef]
89. Fanggao, C.; Saunders, G.A.; Wei, Z.; Almond, D.P.; Cutroni, M.; Mandanici, A. The effect of hydrostatic pressure and temperature on the frequency dependencies of the a.c. conductivity of ionic ($AgPO_3$) and $(Ag_2S)0.3(AgPO_3)_{0.7}$ glasses. *Solid State Ion.* **1998**, *109*, 89–100. [CrossRef]
90. Angell, C.A. Recent developments in fast ion transport in glassy and amorphous materials. *Solid State Ion.* **1986**, *18–19*, 72–88. [CrossRef]
91. Wang, Y.; Sokolov, A.P. Design of superionic polymer electrolytes. *Curr. Opin. Chem. Eng.* **2015**, *7*, 113–119. [CrossRef]
92. Rouxel, T. Elastic properties and short-to medium-range order in glass. *J. Am. Ceram. Soc.* **2007**, *90*, 3019. [CrossRef]
93. Aniya, M.; Kawamura, J. Medium range structure and activation energy of ion transport in glasses. *Solid State Ion.* **2002**, *154–155*, 343–348. [CrossRef]